Using Fuzzy SOM Strategy for Satellite Image Retrieval and Information Mining

Yo-Ping Huang[1], Tsun-Wei Chang[2] and Li-Jen Kao[3]
Dept. of Computer Science and Engineering, Tatung University
Taipei, Taiwan 10451
[1]E-mail: yphuang@ttu.edu.tw; [2]E-mail: alan1107@dlit.edu.tw; [3]E-mail: f1086@mail.ccmtc.edu.tw
Frode-Eika Sandnes
Faculty of Engineering, Oslo University College
Oslo, Norway
E-mail: Frode-Eika.Sandnes@iu.hio.no

ABSTRACT

This paper proposes an efficient satellite image retrieval and knowledge discovery model. The strategy comprises two major parts. First, a computational algorithm is used for off-line satellite image feature extraction, image data representation and image retrieval. Low level features are automatically extracted from the segmented regions of satellite images. A self-organization feature map is used to construct a two-layer satellite image concept hierarchy. The events are stored in one layer and the corresponding feature vectors are categorized in the other layer. Second, a user friendly interface is provided that retrieves images of interest and mines useful information based on the events in the concept hierarchy. The proposed system is evaluated with prominent features such as typhoons or high-pressure masses.

Keywords: Satellite Image, Early-Warning System, Genetic Algorithm, Image Retrieval, Relevance Feedback.

1. INTRODUCTION

Satellite images are used in a wide variety of applications. Automatically recognizing objects such as ships, aircraft or even missiles from satellite images were the main objective during the 70's. The commercial and research uses of satellite images is on the increase. For example, weather images sensed by the Geostationary Operational Environmental Satellite (GOES) are used for tracking hurricanes and storms. Landsat images are used in global change studies such as analyzing deforestation in the Amazon River Basin.

Advanced remote sensing technologies involve huge satellite image datasets that amount to many Tera bytes. Manual management and search in such data are very impractical. The demand for efficiently searching and discovering knowledge in such scientific data is growing. Especially, an efficient retrieval of desired objects in the satellite images can lead to the discovery of certain events that can give an early warning for emerging disasters. This is exemplified in the following scenario. To automatically find a cloud layer, a high-pressure mass or a typhoon is helpful for environmental monitoring, disaster management or early-warning announcement. The urgent need to manage huge quantities of satellite images is the motivation behind the image retrieval and information discovery strategy discussed herein.

Content-based image retrieval (CBIR) techniques based on low-level image content features provides a powerful approach to image retrieval. Several strategies for making satellite image content-based queries had been proposed [1-3]. Most of the CBIR techniques extract significant features from the satellite images to construct image-related feature vectors and then store these feature vectors in a database. Thus, the search for target images involves comparing the feature vectors of the query with the database images. A similarity measurement is computed to determine how visually similar the images in the database are to the query image. Moreover, with the help of query-by-example (QBE), the users can search for target images by providing an individual or multiple examples. Unfortunately, such retrieval strategies occasionally yield unsatisfactory matches. One reason for this is that the feature vectors of some semantic irrelevant images may happen to be close to the query vector in feature space while the feature vectors of the semantic relevant images may be further away. This problem is even more evident when searching for specific objects in a satellite image. This paper proposes a solution to this problem. A framework for efficiently retrieving specific objects is proposed where data are mined from a set of weather satellite images using self-organization maps (SOM). Time-dependent association rules are then extracted. The efficiency of the proposed strategy is experimentally verified using a set of weather satellite images.

The remainder of this paper is organized as follows. Section 2 introduces the satellite image segmentation strategy and the key content features. Section 3 describes the theoretical fundamentals for the proposed image retrieval strategy. Section 4 introduces inter-transaction data mining. Experimental results are discussed in section 5. Finally, conclusions and future research issues are

presented in section 6.

2. SATELLITE IMAGE SEGMENTATION AND FEATURE EXTRACTION

The purpose of satellite image segmentation is to discriminate meaningful portions in a satellite image. Satellite images are partitioned into a set of separate regions [4]. Each region is labeled and characterized to reflect the local structure in the image.

The proposed satellite image retrieval strategy focuses on the content properties of a satellite image. Several content features are extracted including color and shape moment. Several descriptive statistics are used to capture characteristics of essential content features such as mean, variance, and higher order moments.

Color Feature

Color information is important. The hardware-based RGB color model is not perceptually uniform as it is ambiguous for colors such as yellow and green. The RGB color coordinate system can be linearly transformed to the HLS color coordinate system [5]. Here, the L component represents the pixel intensity degree. The H and S components indicate the hue and saturation of the image, respectively.

The color histogram can be used for retrieving images. The color distribution of an image can be represented by different quantities of histogram bins. And each histogram bin will reflect a coarse color range in the color space. As this strategy is invariant to rotation and translation, the color histogram technique is used in the satellite image retrieval system. However, color histograms are sensitive to noise. Two similar colors are viewed as identical if they are positioned in the same bin. On the other hand, two similar colors in different bins caused by a small change of illumination will be viewed as different. Second, histograms have a high dimensionality. The number of dimensions is proportional to the number of bins and consequently the required computational effort. Finally, spatial information is lost when constructing the color histograms. Therefore, to retain spatial relations, statistical histogram descriptors are employed.

Given a satellite image I_A, let Z_i denote a random gray level and $H_{Z_i}^{I_A}$, $i = 0,1,...,L-1$ be the corresponding i-th gray histogram bin for a satellite image I_A, where L is the maximum gray level. Each bin records the amount of corresponding gray value of pixels. To speed up the computation, the gray levels are reduced from 256 to 32 levels. This is sufficient for representing distinct gray levels. The mean value m of gray levels (average gray level) is:

$$m = \sum_{i=0}^{L-1} Z_i \times H_{Z_i}^{I_A}. \tag{1}$$

The evaluation of histogram gray level moments provides an overview of the data rather than an exact comparison.

Shape Features

The proposed strategy employs spatial moments to represent a region. The color image is first converted into a gray image. For a 2-D digital image $f(x, y)$, the moment (m_{pq}) of order ($p+q$) is uniquely determined from $f(x, y)$ [5]. The central moments are defined as follows.

$$\mu_{pq} = \sum_x \sum_y (x - \bar{x})^p (y - \bar{y})^q f(x, y),$$

$$\text{where} \quad \bar{x} = \frac{m_{10}}{m_{00}} \quad \text{and} \quad \bar{y} = \frac{m_{01}}{m_{00}}. \tag{2}$$

The central moments of orders up to 3 are derived as follows.

$$\mu_{00} = m_{00},$$
$$\mu_{01} = 0,$$
$$\mu_{02} = m_{02} - \bar{y}m_{02},$$
$$\mu_{03} = m_{03} - 3\bar{y}m_{02} + 2\bar{y}^2 m_{01},$$
$$\mu_{10} = 0,$$
$$\mu_{11} = m_{11} - \bar{y}m_{10},$$
$$\mu_{12} = m_{12} - 2\bar{y}m_{11} - \bar{x}m_{02} + 2\bar{y}^2 m_{10},$$
$$\mu_{20} = m_{20} - \bar{x}m_{10},$$
$$\mu_{21} = m_{21} - 2\bar{x}m_{11} - \bar{y}m_{20} + 2\bar{x}^2 m_{01},$$
$$\mu_{30} = m_{30} - 3\bar{x}m_{20} + 2\bar{x}^2 m_{02}. \tag{3}$$

The normalized central moments are defined as follows.

$$\eta_{pq} = \frac{\mu_{pq}}{\mu_{00}^\gamma}, \tag{4}$$

where $\gamma = \frac{p+q}{2} + 1$, for $p+q = 2,3,....$

Finally, a set of seven invariant moments can be derived from the second and the third moments as follows.

$$\Phi_1 = \eta_{20} + \eta_{02},$$
$$\Phi_2 = (\eta_{20} - \eta_{02})^2 + 4\eta_{11}^2,$$
$$\Phi_3 = (\eta_{30} - 3\eta_{12})^2 + (3\eta_{21} - \eta_{03})^2,$$
$$\Phi_4 = (\eta_{30} + \eta_{12})^2 + (\eta_{21} + \eta_{03})^2,$$
$$\Phi_5 = (\eta_{30} - 3\eta_{12})(\eta_{30} + \eta_{12})$$
$$[(\eta_{30} + \eta_{12})^2 - 3(\eta_{21} + \eta_{03})^2]$$
$$+ (3\eta_{21} - \eta_{03})(\eta_{21} + \eta_{03})$$
$$+ [3(\eta_{30} + \eta_{12})^2 - (\eta_{21} + \eta_{03})^2],$$
$$\Phi_6 = (\eta_{20} - \eta_{02})[(\eta_{30} + \eta_{12})^2 - (\eta_{21} + \eta_{03})^2]$$
$$+ 4\eta_{11}(\eta_{30} + \eta_{12})(\eta_{21} + \eta_{03}),$$
$$\Phi_7 = (3\eta_{21} - \eta_{03})(\eta_{30} + \eta_{12})$$

$$[(\eta_{30}+\eta_{12})^2-3(\eta_{21}+\eta_{03})^2]$$
$$+3(\eta_{21}-\eta_{30})(\eta_{21}+\eta_{03})$$
$$[3(\eta_{30}+\eta_{12})^2-(\eta_{21}+\eta_{03})^2]\ . \qquad (5)$$

3. CONCEPT HIERARCHY-BASED IMAGE RETRIEVAL

Constructing the Concept Hierarchy with SOM

Self-organizing maps (SOM) is a data visualization technique originated by Kohonen in 1990 which can reduce the dimensions of data. Humans cannot easily visualize high dimensional data. The SOM is trained through the use of iterative unsupervised learning to produce a feature map from the input data to the output space such that the topological properties of this network is preserved. In other words, similar n-dimensional data are grouped together and projected onto grids of the output layer. Each input is connected to all output neurons. Every neuron is associated with a weight vector with the same dimensionality as the input vectors. When input data (query issued by users) is given to the network, its Euclidean distance to all weight vectors can then be computed. The distance on the competition grids implies a similarity between the input data such that the pattern recognition can be completed.

A satellite image comprises its segmented regions which roughly correspond to some specific events. All the database image regions are classified into different categories such as high-pressure mass, cloud layer, linear cloud and typhoon. These categories are used to construct the first layer of this concept hierarchy. Meanwhile, the time-stamp of each event is also logged in the database and its corresponding feature vector is stored in the bottom layer of the hierarchy as shown Fig. 1.

In the proposed strategy, the SOM clusters the conceptual similar regions based on their local features including color and shape moments. The satellite image search is then performed through the concept hierarchy. The Euclidean distance L_2 measures the similarity between the feature vectors. The distance between a region in the query image and the weight vectors of classes is computed to determine which class the region belongs to. The dissimilarity between the region feature vectors and the feature vectors of other regions inside this class is then computed as follows.

$$d(QR_i, TR_j) = \sum_{k=1}^{n} I \times (V_k^{QR_i} - V_k^{TR_j})^{1/2}\ , \qquad (6)$$
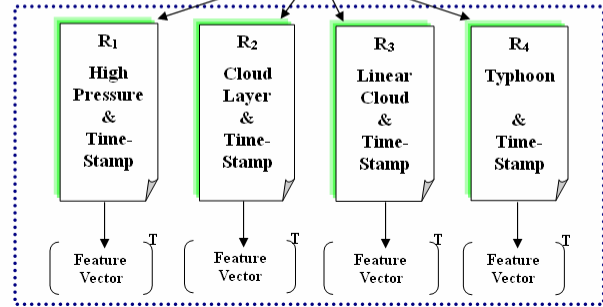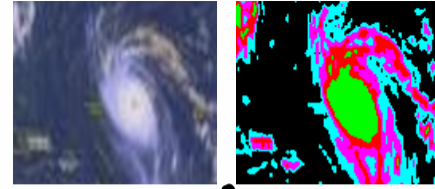
Fig. 1. A weather image is segmented into several regions which are classified into different categories.

When constructing the concept hierarchy, the image ID associated with events and the corresponding time-stamps are logged in the database shown as Table 1. According to the event occurrence table, we can later identify when events happened. The necessary information, such as that in Fig. 2, is then easily retained.

Table 1. The recognized events associated time-stamp and image ID for each satellite image are stored in the database.

Image ID	Time-Stamp	Events
I_1	t_1	a, b
I_2	t_2	a, b, c
.	.	.
.	.	.
I_k	t_k	a, c

4. INTER TRANSACTION DATA MINING

Generating Mega-Transactions

The dimensional attribute D is used to describe the properties associated with the items including time and location. Assume the domain $Dom(D)$ of the dimensional attribute D is ordinal which can be separated with equal length intervals. For example, the time intervals could be one day, a week, a month, etc. These intervals are represented by integers 0, 1, 2, respectively, without loss of generality.

There is an inter-transaction association rule that spans across m intervals when an association of m intervals apart between items. Basically, an inter-transaction association rule can cross multiple intervals. Nevertheless, two reasons are considered: 1) it will take considerable computation time to find all rules, 2) users may not be interested in the rules spanning more than a certain number of intervals; a sliding window w is employed to reduce the computational effort. When mining

inter-transaction association rules, only the rules spanning less than or equal to w intervals will be taken into consideration. This is exemplified in Fig. 2. A transaction database has a dimensional attribute of occurrence day. There are five transactions located at intervals 1, 3, 6, 9, and 11. While the length of the sliding window is 4, we will get five sliding windows $W1$, $W2$, $W3$, $W4$, and $W5$, with addresses of 1, 3, 6, 9, and 11, respectively. The sub-window $W1[0]$ contains items a, b, e and g and the sub-window $W1[3]$ contains c, f, and i. Each sliding window generates a mega-transaction. A mega-transaction M contained within W is denoted as follows.

$$M = \{i_k(j)\,|\,i_k \in W[j]; 1 \le k \le u; 0 \le j \le w-1\}; \qquad \text{where}$$

W is a sliding window with w intervals and u is the number of items in the itemset $I = \{i_1, i_2, ..., i_u,\}$.

| Occurrence Day	Events
1	a, b, e, g
2	
3	c, f, i
4	
5	
6	a, e, d, h
7	
8	
9	a, e, d
10	
11	b, c, f
12	
13	
14	
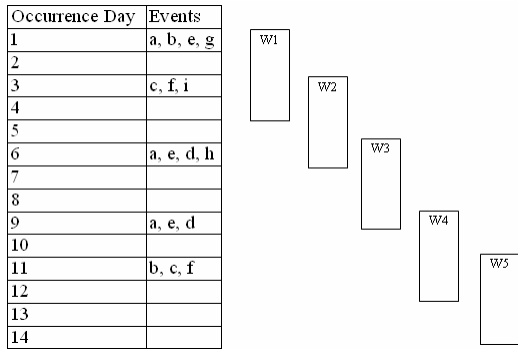
Fig. 2. A transaction database with a sliding window of 4 intervals.

The mega-transaction in $W1$ is $\{a(0); b(0); e(0); g(0); c(2); f(2); i(2)\}$. To distinguish the items in a mega-transaction from the items in a conventional transaction, the items in a mega-transaction are called extended items. The set of all possible extended items is denoted $I^{'}$. Given I and w, we have

$$I^{'} = \{i_1(0),...,i_1(w-1), i_2(0),...,i_2(w-1),...,i_u(0),...,i_u(w-1)\}$$

Let T_{xy} be the set of mega-transactions that contains a set of extended items $X \cup Y$ and T_x be the set of mega-transactions that contains X. Let S be the number of mega-transactions in the transaction database. Then, the support and confidence of an inter-transaction association rule $X \Rightarrow Y$ are defined as follows.

$$\sup port = \frac{|T_{xy}|}{S}, \qquad confidence = \frac{|T_{xy}|}{|T_x|}. \qquad (7)$$

Our goal is to discover inter-transaction rules from the transaction database with support and confidence greater than or equal to the predefined requirements.

Generating Inter-Transaction Association Rules

The proposed inter-transaction association rules' mining is composed of two steps.

1. Finding the frequent inter-transaction itemsets which are all the inter-transaction itemsets with support higher than minsup.
2. Generating the association rule $X \Rightarrow (F - X)$ for every frequent inter-transaction itemset F and all possible combinations of $X \subset F$ while all of the following conditions are satisfied.
   a. $\exists i_k(0) \in X$, $1 \le k \le u$.
   b. $\exists i_k(j) \in (F - X)$, $1 \le k \le u$, $j \ne 0$.
   c. Confidence of $X \Rightarrow (F - X)$ is higher than minconf.

The first step is the bottleneck while generating inter-transaction association rules. This is mainly because the number of extended items in I' is w times the number of items in I. Consequently, more candidate inter-transaction itemsets are generated. A significant computational effort is required to compute the support of candidate inter-transaction itemsets. On the other hand, step 2 incurs less computation effort. The Apriori algorithm [6] was adopted and modified to conduct step 2. Assume that the database has only one quantitative attribute, i_j, where $1 \le j \le k$. If i_j is mapped to l fuzzy intervals, the new set of all items I_f would be $\{i_{(1, B)}, i_{(2, B)}, ..., i_{(j, 1)}, i_{(j, 2)}, ..., i_{(j, l)}, i_{(j+1, B)}, ..., i_{(k, B)}\}$, where $i_{(r, B)}$, $r \ne j$, is a binary attribute and $i_{(j,s)}$, $1 \le s \le l$, is a fuzzy attribute. Now, the mega-transaction M contained within W can be redefined as follows.

$M = \{i_{(j, x)}(t)|\ i_{(j, x)} \in W[t], 1 \le j \le k, x$ is the literal B if it is a binary attribute, else $1 \le x \le l$ if it is a fuzzy attribute, $0 \le t \le w - 1\}$.

The set of all possible extended items can be redefined as follows.

$I'_f = \{i_{(1, B)}(0), ..., i_{(1, B)}(w - 1), i_{(2, B)}(0), ..., i_{(2, B)}(w - 1), ..., i_{(j, 1)}(0), ..., i_{(j, 1)}(w - 1), ..., i_{(j, l)}(0), ..., i_{(j, l)}(w - 1), i_{(j+1, B)}(0), ..., i_{(j+1, B)}(w - 1), ..., i_{(k, B)}(0), ..., i_{(k, B)}(w - 1)\}$.

Now, we could continue to find frequent itemsets. An inter-transaction k-itemset is the set $B = \{i_{(1, x)}(t_1), i_{(2, x)}(t_2), ..., i_{(k, x)}(t_k)\}$, where $B \subseteq I'_f$ such that $\exists i_{(j,x)}(0) \in B$, $1 \le j \le k$.

The Apriori algorithm can be used to find the frequent itemsets while performing level-wise mining, i.e., using inter-transaction frequent k-itemsets (for $k \ge 2$) to generate the candidate $(k+1)$-itemsets as follows.

Step 1. Discover the frequent 1-itemset L_1. Actually, I'_f is the candidate 1-itemsets C_1 which is the set of all possible extended items. This can be done by scanning the database of mega-transaction T_1 to determine whether a special item $i_{(j,x)}(t)$ exists. If it does, for a binary attribute increases the count of $i_{(j,x)}(t)$ by 1, otherwise for a fuzzy attribute calculate its membership degree. After the database has been

scanned once, L_1 can be found.

Step 2. Generate the 2-item candidate set from L_1. The 2-item candidate set is of the form $C_2 = \{\{a(0), b(t)\}|\ a(0), b(t) \in L_1,\ (t = 0 \wedge a < b)$ or $(t \neq 0)\}$. Note that a, b cannot be fuzzy attributes from the same quantitative attribute simultaneously.

Step 3. Since most 2-item candidates appear in C_2, the C_2 must be downsized before L_2 is generated. We first hash all 2-itemsets in C_2 like $\{a(0), b(t)\}$, $t \neq 0$ in the current transactions into its corresponding buckets of a hash table. The 2-itemsets from C_2 with corresponding bucket count less than the minsup are pruned. A valid k-itemset B's support value sup is calculated as follows.

$$\text{sup}(B) = \prod_{i_{(j,x)} \in B} \mu(i_{(j,x)}), \text{ where } \mu(i_{(j,x)}) = 1, \text{ if } i_{(j,x)}$$

is a Boolean attribute; otherwise $\mu(i_{(j,x)})$ equal its membership degree for a fuzzy attribute.

Step 4. Discover the frequent 2-itemset L_2 by applying the Apriori algorithm to C_2.

Step 5. Generate the k-item candidate set C_k and discover the frequent k-itemset L_k, where $k > 2$. Given L_{k-1}, we can get C_k by joining L_{k-1} with L_{k-1}. All itemsets $B \in C_k$ that have $(k-1)$-subsets with support less than the minsup are deleted in the pruning phase.

Step 6. Repeat step 5 until no more frequent itemsets can be found.

Step 7. Generate the inter-transaction association rules. The inter-transaction association rules can be produced just as the generation of conventional association rules except that the confidence is calculated according to $\dfrac{\text{sup}(xy)}{\text{sup}(x)}$, where $\text{sup}(xy)$ is the support value for the itemset that contains a set of items $X \cup Y$. The $\text{sup}(x)$ is the support value for itemset containing items X.

5. EXPERIMENTAL RESULTS AND DISCUSSIONS

A satellite image retrieval system has been implemented to verify the effectiveness of the proposed strategy. A set of 100 satellite images was downloaded from the Central Weather Bureau of Taiwan consisting of objects including high pressure, cloud layers, linear clouds and typhoons. These satellite images were first segmented into five regions.

The first experiment is carried out to evaluate the effectiveness of the proposed model. The returned images are considered relevant once they appear in the same category to the query; and the precision rate can be derived from the computation of how many relevant images are returned in a retrieval round. For the first experiment, a satellite image with clouds around Taiwan

is used as the query and the retrieval results are shown in Fig. 3. The proposed model has the ability of accessing partially similar regions in a satellite image. There are 4 matches among the top 5 returned images from the database and an 80% precision is obtained. There are two high-pressure zones occurring in the 3rd satellite image; actually, the 3rd image is also similar to the query to some extent. That is, the top 5 returned satellite images contain a portion of similar regions to the query. Nevertheless, the interpretation of identified objects in a satellite image is highly depending on the domain experts. The identification of objects is helpful for future analysis and discovery of useful information from satellite images.

In the second experiment the inter-transaction association rule mining was applied to the satellite events logged in the database. Table 2 listed the current used events.

Table 2. The events used for current work.

Event	Meaning
TY	Typhoon
LC	Linear Cloud
HP	High-Pressure Mass
CL	Cloud Layer

From the events logged in the database, the occurring events are transformed as shown in table 3. The binary value 1 indicates that the corresponding event happened on that day, while 0 represents that the event did not occur on that day. The proposed inter-transaction association rule mining can be then applied onto the data in table 3. The partial mining results are demonstrated in table 4 while different window lengths are used in mining the inter-transaction association rules as shown table 4. While using 3 intervals as the window length, one association rule indicates that the linear cloud occurred in the first day and the cloud layer occurred next day, then the typhoon occurred the following two days. While using 6 intervals as the window length, one association rule indicates that the high-pressure mass occurred on the first day, the linear cloud occurred the next day, the cloud layer occurred the following two days and the high-pressure mass occurred the following four days, then the typhoon occurred the following four days.

Table 3. The transformation from satellite events into binary values.

Day	TY	LC	HP	CL
1	1	1	0	1
2	1	1	0	0
3	0	0	0	1
…	…	…	…	…

Table 4. The results of inter-transaction association rules mining.

	sliding window length = 3 intervals.	sliding window length = 6 intervals.
Partial	<LC(0), CL(1), TY(2)>	<HP(0), LC(1), CL(2),

results		HP(4), TY(4)>
Elapsed Time	5.95sec	8.81sec

6. CONCLUSIONS AND FUTURE WORK

In this paper, a SOM-based satellite image retrieval model was proposed to retrieve satellite images according to the corresponding features in query satellite images. The experimental results demonstrate that the SOM-based image retrieval approach achieved good retrieval accuracy. Satellite images are found by considering different categories. Both query-by-example approach and query-by-region techniques were employed to achieve the retrieval. Minimal feature set was used to characterize a region in a satellite image. The experimental results verified the efficient accessibility of satellite images. Nevertheless, the automatically extracted low-level features cannot fully capture the semantics of satellite image content. Therefore, the discriminative approach associated with semantic relationships is indispensable to capture more aspects of satellite images.

In addition, inter-transaction association rules mining was introduced to predict specific events. The proposed data mining algorithm for satellite images can remove highly similar data sequences to reduce the computational effort. While generating k-item candidates and counting support values for each itemset are time-consuming, the hash-based technique is proposed to help reduce the computational complexity.

CBIR technique is a solution for effective searching and browsing of large satellite image archives. There is a rapid growth and availability of remote sensing images. Rich satellite image contents make the retrieval task even more challenging. The current approach can be extended to enhance the performance of satellite image retrieval. The current work did not consider the spatial relationship between events (regions in our case). More additional low level features can be adopted to better represent content semantics. The definition of inter-transaction association rules has to be extended as multi-dimensional inter-transaction association rules. The extension can present more valuable spatio-temporal information in satellite images.

REFERENCES

[1] G.L. Heileman and Y. Yang, "The Effects of Invisible Watermarking on Satellite Image Classification," **Proc. of the 3rd ACM Workshop on Digital Rights Management,** 2003, pp.120-132.

[2] Y. Li and T.R. Bretschneider, "Semantics-based Satellite Image Retrieval Using Low-level Features," **Proc. of IEEE Int. Geoscience and Remote Sensing Symposium**, Vol. 7, 2004, pp.4404-4409.

[3] Y. Li and T.R. Bretschneider, "Semantic-Sensitive Satellite Image Retrieval," **IEEE Trans. on Geoscience and Remote Sensing**, Vol. 45, Issue 4, April 2007, pp.853-860.

[4] Y.-P. Huang and T.-W. Chang "A Fuzzy Inference Model for Image Segmentation," **IEEE Int. Conf. on Fuzzy Systems**, May 2002, pp.972-977.

[5] R.C. Gonzalez and R.E. Woods, **Digital Image Processing**, Prentice-Hall, Inc. Pub., Second Edition, New Jersey, 2002.

[6] R. Agawal and R. Srikant, "Fast Algorithms for Mining Association Rules," **Proc. Int. Conf. Very Large Data Bases**, September 1994, pp.487-499.

(a)   (b)
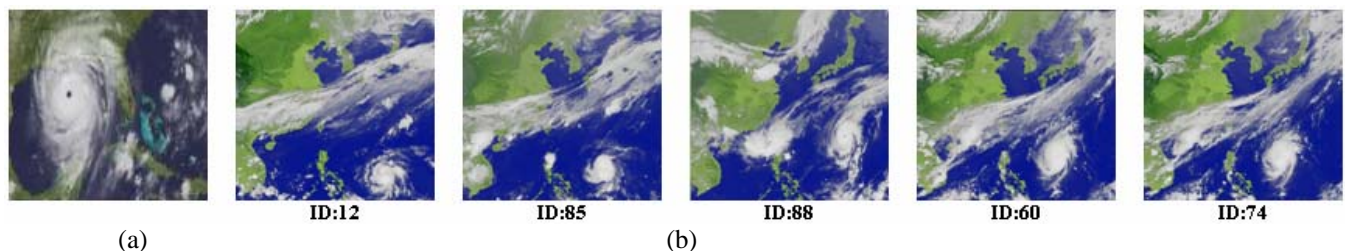
Fig. 3. (a) The query image is not in the database, (b) the retrieval results ranking from left to right.